How does climate change affect the decline of an alpine plant population?

Caleb Christian

Mentors: Nora Underwood, Brian Inouye

Full-time independent research/REU

2026

Abstract

Alpine ecosystems face rapid climate change, yet long-term demographic responses to this change remain understudied. Long-lived alpine monocarpic plants like *Tetraneuris grandiflora* may be vulnerable to environmental volatility. While warming and snowpack changes impact plant vital rates, few studies examine how lagged climate effects compound over decades to create population trends. We investigate how historical climate variation drives the multi-decadal decline of a population of *T. grandiflora* at the Rocky Mountain Biological Laboratory. Using 47 years of individual-based census data (1979-2025), we parameterized size-structured integral projection models (IPMs) featuring a recruit bank. We combined automated global selection for climatic effects with stochastic simulations, temporal hindcasting, and elasticity perturbation analysis across historical and modern climate regimes. Incorporating climate in IPMs substantially improved predictive hindcasting ability, especially when initiated in 1996 at the start of the population's decline. (RMSE decreased from 0.455 to 0.363). Stochastic projections confirmed a transition from population growth under the historical climate ($\lambda_{s=}$1.002 under 1979-1995 climate) to a shrinking population under the current climate (λ_s=0.946 under 1996-2025 climate). Modern climatic conditions amplified reliance on adult survival (elasticity rising from 0.179 to 0.278). Our findings demonstrate that modern climatic conditions create a situation where adult survival is more important to the population while also hurting adult survival.

Introduction

Climate change can cause a multitude of species-specific effects on alpine plant populations (de Valpine and Harte 2001, Grabherr et al. 2010, Inouye 2020). Because of the stark elevation gradient that is present in alpine ecosystems, alpine plant communities face typical climate-change related problems as well as threats from vertical shifts in species distributions (Matteodo et al. 2013, see Freeman et al. 2018 for an example in avian communities). Plants may also suffer from evolutionary trade-offs under climate change that cause the populations to be unable to reach a fitness maximum (Williams et al. 2015). Despite predicted robustness in alpine plant populations to climate change (Körner and Hiltbrunner 2021), alpine plant communities are generally declining in abundance, richness, and quality of plants (de Valpine and Harte 2001, Lesica and McCune 2004, Inouye 2020), leading to the need of species-specific alpine plant research.

Some common mechanisms of physiological change under climate change include a less robust snowpack that creates a less-insulated environment for alpine plants and promote early growth that is destroyed by frost events (Edwards et al. 2007, Palacio et al. 2015, Kosolapova and Altshuler 2024). Specifically, snowmelt disturbances caused by climate change lead to decreases in survival rates, oftentimes the primary driver of population growth and decline in alpine perennials (Iler et al. 2019a). Furthermore, the increased duration of warm growing season for alpine plants is unlikely to overcome the predicted and realized decrease in snow pack from climate change (Wipf et al. 2009, Kotlarski et al. 2023). This can cause a loss of community diversity through local extirpation, including functional diversity, which can disrupt ecological processes and ecosystem functions (Cadotte et al. 2011). Thus, documenting and analyzing the changing demographics of alpine plant populations can increase our understanding of at-risk alpine ecosystems and how climate change is affecting these populations (Inouye 2020). There have been several studies documenting how climate affects plant population demographics and their effects on growth rates (Dalgleish et al. 2011, Tenhumberg et al. 2018, Oldfather and

Ackerly 2019), but few have examined climatic effects in parallel with a declining alpine plant population and long-term demographic data.

Most alpine plants are long lived with low fecundity rates (Billings and Mooney 1968), and thus robust population models require longer datasets (Fieberg and Ellner 2001, Che-Castaldo and Inouye 2011). When modeling populations that are age or stage structured, such as alpine plants, traditional age-independent population models fail to capture differences in the survival and reproductive ability of different ages or stage classes (Caswell 2006). It is common in conservation, management, and academic settings to use matrix population models (MPMs) in order to consider the demography of population dynamics (Caswell 2006). However, MPMs are often biologically unrealistic due to the discrete stages that ignore intra-stage variation (Easterling et al. 2000, Merow et al. 2014). To overcome this problem, integral projection models (IPMs) treat size as a continuous variable (Easterling et al. 2000, Merow et al. 2014), yielding more biologically realistic predictions that require less data for reliable estimations (Merow et al. 2014).

Tetraneuris grandiflora (previous genus: *Hymenoxys*), commonly known as “Old Man of the Mountain,” “Four-Nerved Daisy,” or “Alpine Sunflower,” is a monocarpic alpine sunflower that can live 10-20 years (National Park Service 2024). There is a currently declining population near the Rocky Mountain Biological Station (RMBL) that has long-term demographic data. There have been other studies linking climate change to changing demography and decreased population abundances across taxa (Kagawa et al. 2024, Andrzejak et al. 2025), but we still do not have generalizable mechanisms of how these phenomenon occur (Campbell 2019). Thus, studying the population dynamics of the species is useful not only to describe the life history of the species, but also to use a model species to demonstrate how climate affects a declining alpine plant population.

We seek to understand how climate variables have impacted demographic changes in *T.* grandiflora, especially in the context of the population’s decline. We have two hypotheses for this study. First, we hypothesize that climate change will decrease the growth rate of the population through changing vital rates. We also hypothesize that climate change will change the elasticities of the population, which will change the sensitivity landscape of the population. We predict both of these will decrease the growth rate of the population.

Methods

Study Species and System

T. grandiflora is a long-lived monocarp, meaning it flowers once and dies. It is an alpine sunflower species (*Asteraceae* family) that is found throughout the Rocky Mountains of the western United States. It grows in subalpine and alpine environments. There has been little ecological study of *T. grandiflora* (but see Oberbauer and Billings 1981, Winkler et al. 2018). David Inouye has annually censused a population of *T. grandiflora* in Virginia Basin, CO, USA (N38º58.690', W106º58.562', 11,300 ft elevation), since 1979. The population steadily rose in size until approximately 1995 and has since been steadily declining, with a large drop in population size from 1995-1996.

Demographic Censusing

David Inouye has annually censused a population of *T. grandiflora* in Virginia Basin since 1979, recording the number of leaves and the length of the longest leaf (LLL), using a metal tag system to identify plants. There are three parallel 1m x 20m plots that are separated by one meter (Figure 1). Censuses are typically performed in early August when plants are flowering, but dates range from July 26th to September 2nd. We constructed a clean dataset that also contains survival of the following year, the number of leaves the previous year, the LLL the previous year, and the number of aborted buds (starting in 1990). For years in which a plant was not found but was found in following years, the number of leaves and the LLL were coded as "NA". If a plant was flowering, the number of leaves and LLL were not recorded. Comments left by the original field observers are included in the cleaned dataset. To resolve ambiguous data entry, we consulted with D.W. Inouye and the original paper data sheets.

Empirical Population Analysis

In order to find the empirical λ of the population, we first plotted the natural logarithm of the raw population size over time. Because there was a change in the dynamics of the species in 1995-1996 (see Figure 2), we calculated λ from 1979-1995 and from 1996-2026 to maintain linearity in our calculation of λ. We used a linear model of form $\ln\left(N_t\right)=\ln\left(N_0\right)+t\cdot\beta$, which we extracted λ from using $\lambda=e^{\beta}$.

Regressions

Because IPMs are continuous extensions of MPMs, they can be parameterized using regressions that are widely used by ecologists (Easterling et al. 2000, Merow et al. 2014). We used the package 'glmmTMB' (Brooks et al. 2017) in R version 4.5.1 (R Core Team 2025) to build and run regression models. To take advantage of having two size measurements, we applied a square-root transformation to the number of leaves to linearize its relationship with LLL (r = 0.79), then z-scaled both variables and summed them to create a composite size metric. Following the guide created by Merow et al, we used logistic regression for size-specific probabilities of survival and reproduction. Exploratory analyses indicated a nonlinear size-survival relationship, so we included a quadratic term for the survival model, which was significant. For the number of flowers a plant produces given reproduction, we used count regression with a Poisson distribution. For plant growth, we followed Miller and Ellner's guide to building growth models for IPMs and used Student's t-regression with nonconstant variance due to leptokurtic distributed growth (Miller and Ellner 2025).

To consider the effects of climate, we used separate regressions following the same formats but using climate variables collected in Gothic, CO (Prather et al. 2023). We acknowledge that this data is collected lower in elevation and a short distance away from the study site, but due to the longevity of data available and the similar environments we do not anticipate qualitative differences in results from it. We used spring mean temperature, summer mean temperature, and snowpack fallen overwinter as our climate variables, except for recruit size distribution which we used snowmelt date to capture the amount of growing season available to recruits. We z-scaled all our climate variables prior to analysis. To consider lagged

climatic effects on vital rates (Evers et al. 2021), we used automated global selection from the 'MuMIn' package (Bartoń 2026), allowing up to three climatic variables per vital rate to prevent overfitting and keeping composite size variables as fixed terms. We selected the best model using Akaike Information Criteria (AICc). All candidate models within $\Delta AIC \leq 2.0$ were considered to have equivalent empirical support (Burnham and Anderson 2002), where all ΔAIC values are in reference to the top-ranked model. When top ranked models were statistically indistinguishable ($\Delta AIC \leq 2.0$), we selected the final model based on fewer lag terms and coefficients consistent with known alpine plant physiology. For example, when two models had equivalent AIC support, we preferred models with earlier or no lags over longer lags, as immediate physiological responses to climate are better established than multi-year carryover effects. When choosing the best model for the number of flowers, the null model (no climate variables) was within $\Delta AIC \leq 2.0$, so we selected the simplest model (only composite size as a predictor). Checking for multicollinearity in all models showed no excessive collinearity between covariates ($VIF < 1.5$ for all covariates). We extracted slopes, dispersions (for relevant models), and intercepts for all covariates of the selected models.

Recruit Distribution

Because of the small size of *T. grandiflora*, seedlings were often not detected in their first year. However, plants often evade detection for longer than just their year as seedlings, leading to a distribution of first-year detected plants that spans almost the full-size range. To identify plants that were actually 2-year-old recruits, we estimated the maximum size a two-year recruit could be using the growth regression.

There were four plants that were identified as seedlings during data collection. We took the mean and variance of the composite sizes of these seedlings and projected the maximum size possible using 95th percentile growth, accounting for the t-distribution and nonconstant variance used in the growth model. We used average climate variables for this forward projection. All first-year detected plants larger than this maximum size for a year-two plant were considered non-recruits and discarded from further recruit distribution analysis.

We used snowmelt day from the current and previous year as predictors for recruit size. We extracted the slopes of the covariates and the standard deviation of recruit size distribution.

Population Dynamics Models

IPMs generally consist of a fecundity kernel, $F(z',z)$, and a survival/growth kernel, $P(z',z)$, which are combined into the general kernel $K(z',z) = F(z',z) + P(z',z)$, with z being size at time t and z' being size at time t+1. (Easterling et al. 2000, Ellner and Rees 2006). These kernels are integrated over $\Omega = [L, U]$, the set of possible sizes, which is generally increased by 20% to prevent eviction (Merow et al. 2014). The simple IPM is given by

$$n_{t+1}(z') = \int_{L}^{U} K(z',z)\, n_t(z)\, dz$$

for a simple, deterministic, density-independent IPM. However, because of *T. grandiflora*'s small size, seedlings are often not detected. Therefore, we cannot accurately calculate the distribution of seedlings entering the population and had to use a general IPM (Ellner and Rees 2006, Ellner et al. 2016a). We modified a previous IPM with a seed bank (Ramula et al. 2009) to include a recruit bank (RB) that has a maximum residence of one year. Plants move from the main population to the recruit bank through fecundity, then back to the main population. Because *T. grandiflora* is monocarpic, we include the complement of the probability of flowering for a given size to automatically remove flowering individuals from the survival/growth kernel (Metcalf et al. 2003). The modified model is presented below:

$$RB_{t+1} = g \cdot s_1 \int_L^U p_f(z,C) \cdot f_{se}(z) n_t(z) dz$$

$$n_{t+1}(z') = RB_t \cdot f_1(z',C) \cdot s_2 + \int_L^U P(z',z,C) \cdot n_t(z) dz$$

$$P(z',z,C) = s(z,C) \cdot (1 - p_f(z,C)) \cdot G(z'|z,C)$$

with all new variables defined in Table 1. We implemented this model using the R package 'ipmr' (Levin et al. 2021) using a general, density-independent, stochastic, kernel-resampled model. When a vital rate had a time-lagged climate effect, we used the time-lagged climate as the climate vector for the current year's kernel (same year if time lag was 0). For the null IPM, we used the mean climate for all climatic variables. However, because the variables were on a z-scale, these mean values were 0 and vital rates were only dependent on composite size. We used 100 mesh points, with sequential historical years 1979-2025 in chronological order for the kernel sequence. We calibrated our estimated parameters such that our climate IPM λ_s matched the empirical λ from 1996-2026 to find a demographic baseline. We used the same estimated parameters for every subsequent IPM.

After constructing the respective IPMs, we obtained stochastic lambda values (Rees and Ellner 2009). We could also use the discretized kernels to obtain sensitivity values and then elasticity values for our different vital rates (Caswell 2006). Because analytical sensitivity and elasticity analysis is difficult with stochastic IPMs, we performed parameter sensitivity analysis on estimated parameters by perturbing them by a small $\delta = 0.05$, rerunning the IPM, then measuring the change in lambda. To measure the change in λ, we first ran the IPMs with unperturbed parameters to calculate a baseline λ. We ran three elasticity analyses with the same δ perturbation. One analysis included a mean climate and two including randomly drawn climate variation from the 1979-1995 and the 1996-2025 climates across 200 iterations to capture the effects of environmental stochasticity, given the current climatic regime (see Figure 3), on the elasticities of different vital rates. The two climate regimes were differentiated by 1996. The historical climate regime had more snow that melted later and was cooler compared to the modern climate regime. We sampled years with replacement from the 1979-1995 and 1996-2025 climates to avoid analyzing transient dynamics resulting from the initial population size in 1979 (Tuljapurkar 1990).

To understand the effect of climate on the IPM, we compared the annual λ values of the stochastic null IPM and climate IPM through time. We also hindcasted the population size using both the null and climate IPM from the empirical 1979 size distribution, with an estimated

number of individuals in the recruit bank of 10. We then compared the population sizes from the empirical dataset, the null IPM, and the climate IPM using root mean square error (RMSE) to measure how well the models predicted the empirical population size, with a lower RMSE indicating better model fit. We used the logarithm of the population size.

Because of the switch in 1995-1996 from increasing population size to decreasing population size shown in Figure 1, we also initiated a climatic IPM beginning in 1996 to attempt to better predict the exact decline of the population from 1996-2026. Because the climate IPM initialized in 1979 did not exactly match the empirical population size in 1996, we used the empirical 1996 size distribution in an attempt to better predict the population decline period. We also measured the RMSE from the null, climate, and climate post 1996 models' population size to the empirical data.

Results

Empirical Population Size

The empirical population experienced a positive growth rate of λ=1.080 (95% CI: 1.059-1.101) from 1979-1995. From 1995-1996, the population experienced a large decrease in individuals from 233 to 125. Following this drop, the population has been steadily declining since. We found λ=0.953 (95% CI: 0.943-0.962) from 1996-2026.

Regressions and Model Selection

From the automated global selection models, survival and growth had clear best models (ΔAIC=3.14, ΔAIC=9.39, respectively). Reproduction had two models within $\Delta AIC \leq 2$, and the chosen model had 2 same-year terms of spring mean temperature and summer mean temperature. For the number of flowers, there were many models within $\Delta AIC \leq 2$, including the model without any climate variables (Burnham and Anderson 2002, Arnold 2010). The intercepts and slopes are presented in Table 2.

We found that snowpack depth consistently positive and negative effects on vital rates (3-year lag for survival, 4-year lag for reproduction). Spring mean temperatures had a negative correlation with vital rates (4-year lag for survival, no lag for reproduction, 1- and 2- year lag for growth). Summer mean temperatures had mixed correlations with vital rates (1-year lag for decreased survival, no lag for increased reproduction, 2-year lag for increased growth). We found that a later snowmelt date (lag 1 and 2 years) decreased recruit sizes.

Baseline Demography and Elasticity Analysis

Using the same estimated parameters in the null IPM as in the climate IPM to achieve an accurate λ_s compared to our empirical lambda, we found the baseline, mean-climate λ=0.974.

After perturbing each parameter individually, all perturbed vital rates caused λ to increase except for the intercept of probability of flowering. We found a baseline λ=0.984 for the mean climate elasticity analysis. Adult (classified as non-recruits) survival had an elasticity of $e_{survival} = 0.224$, growth had an elasticity of $e_{growth} = 0.103$. Because they are indistinguishable mathematically in the recruit bank equation, germination, the number of seeds, and seedling survival all had elasticities of $e_{constant} = 0.097$. Reproduction had a negative elasticity, $e_{reproduction} = -0.070$. However, we used perturbation on the intercepts of the models, of which reproduction had a negative intercept. Therefore, this negative value is not an indication that more reproduction would lead to a lower λ_s value because the perturbation caused the intercept to decrease rather than increase.

Climate IPM Analysis

We found that our climate IPM (RMSE=0.404) predicted the empirical population size better than our null IPM (RMSE=0.533, see Figure 4). When only considering population size from 1996-2025 when the population was steadily declining, our climate IPM post 1996 (RMSE=0.363) predicted the empirical population size best compared to the full climate IPM (RMSE=0.426) and the null IPM (RMSE=0.455).

Adding environmental stochasticity caused changes in demographic elasticity values. The two climate regimes also yielded different baseline λ_s values ($\lambda_{1979\text{-}1995}$=1.002, $\lambda_{1996\text{-}2025}$=0.946). The 1979-1995 growth climate dampened elasticities compared to the mean climate, while the 1996-2025 modern climate amplified elasticities (see Figure 5). In particular, the *T. grandiflora* population was more dependent on adult survival under the modern climate (elasticity shifted from 0.179 to 0.278). The modern climate also caused reproduction to have a worse effect on the population (elasticity shifted from -0.059 to -0.091), confirming that the modern climate regime penalizes the monocarpic life-history strategy in this population.

Discussion

Collectively, these results provide evidence that the modern climate regime create conditions that push the population towards decline (λ_s<1). By incorporating climate into the stochastic IPM, we were able to better track the multi-decadal population decline of *T. grandiflora* (dropping RMSE from 0.533 to 0.404). When only considering the declining interval of the empirical population (1996-2026), the post-crash IPM predicted the steady population decline better than the null IPM (RMSE dropped from 0.465 to 0.363) and the full-length climate IPM (RMSE dropped from 0.426 to 0.363).

Different climate variables yielded different effects on vital rates. Overwinter snowpack had long lag effects on survival and reproduction (3 and 4 years, respectively). A deeper

snowpack promoted survival and reproduction, likely because of the insulative property of snow prevented thaw-freeze damage (Campbell 2019, Kosolapova and Altshuler 2024). Shown in the length of lag times, these thaw-freeze events were probably not fatal, but instead depleted their carbohydrates reserves and lowered their fitness (Janeček et al. 2015). The converse of this trend with climate change indicates poorer survival and higher reproductive rates in the future. However, due to the negative elasticity of reproduction, these should both push λ down. Spring temperatures had consistently negative effects on vital rates on different timescales. Warm spring temperatures cause premature vegetative growth, exposing tissue to late-season frost events (Inouye 2008, 2020, Iler et al. 2019), which can have aforementioned lagged effects that cause mortality and less growth years later. Warm summer temperatures can elevate vapor pressure deficit, which could decrease survival (Grossiord et al. 2020). However, warm summer temperatures were also associated with increased growth (lag 2 years) and reproduction (same year), contrasting the other negative correlations of climate change on vital rates.

Under the modern climate regime (1996-2025), the growth rate of the population is more reliant on adult survival than under both a mean climate and the historic climate (1979-1995). However, we have shown that climate change trends are decreasing adult survival. Due to the higher adult survival elasticity under the modern climate and lower reproductive elasticity, along with summer temperatures increasing the probability of reproduction, the monocarpy in this population of *T. grandiflora* is partially responsible for their decline in abundance. This could provide a possible mechanism for the decline in alpine plant communities observed.

We found that reinitializing the climate IPM starting in 1996 for hindcasting resulted in less error compared to the climate IPM hindcasted starting in 1979. We used empirical size starting distributions for both hindcasts (Ellner et al. 2016b). Because populations are rarely at a stable size distribution, accounting for empirical population size ensures the early years of the model were governed by empirical transient dynamics (Hastings 2004), not transient dynamics resulting from an erroneous, convenient initial size distribution in the IPM (Fieberg and Ellner 2001, Tenhumberg et al. 2018). Furthermore, to ensure the observed population dynamics from hindcasting were driven by climate rather than the possibility of transient dynamics, from sampling bias or undetected individuals in the recruit bank, or a parameter calibration artifact, we performed long-term stochastic projections under resampled climate regimes. According to stochastic demography theory, repeated sampling across environmental sequences, given enough iterations, burns off initial stage-structure, converging on the asymptotic λ_s via ergodic properties (Tuljapurkar 1990, Ellner et al. 2016b). Because long-term stochastic sampling yielded λ_s=1.002 under the 1979-1995 climate sequence and λ_s=0.946 under the 1996-2025 climate sequence, we confirm the regime shift shown in Figure 3 reflects genuine climate-driven effects, rather than transient dynamics or baseline parameter sensitivity.

While we were able to separate regimes in the IPMs, there were some population abundance events we were unable to explain. The magnitude of the population boom in the early 1990s was unable to be explained by the climate IPMs while also accounting for the long-term

population decline. The high growth rate of λ=1.080 during this period and the inability for the climate models to predict the population increase suggests non-climatic reasons, such as earlier, pre-data collection disturbance or release from limiting factors, for the high λ value. The magnitude of the drop in empirical abundance shown in Figure 1 was not replicated in any IPM. However, there is a notable drop in the climate IPM hindcast population size from 1995-1996, suggesting climate may have confounded with another disturbance to cause the drop. Eventually the climate IPM hindcasts and empirical abundance nearly converged in the early 2010s. In 2025 and 2026, the empirical population had a small recovery in abundance, increasing from 20 individuals to 32 from 2024-2025, whereas both climate IPMs predicted further decline in these years.

Plant communities in the high Rocky Mountains and broader alpine systems are experiencing declines (Inouye 2020, Nomoto and Alexander 2021, Ellis and Shriver 2026), and this population of *T. grandiflora* demonstrates the effect that climate change, particularly differing climate regimes, has in the mechanisms of the declining population. The ability to use 47 years of data to parameterize IPMs, hindcast and verify different IPMs, and split the system into two climate regimes allowed us to disentangle climate lagged effects from short-term population fluctuations, despite their magnitudes. We also emphasize the value in considering a plethora of lagged climatic effects on vital rates with an objective method when constructing a climate-informed population model. Looking forward, alpine plant populations and their vital rates will be affected not just by a warmer mean climate, but also by the increasing environmental variance under climate change (Thornton et al. 2014) as shown by the elasticity analysis.

Figure 1. Map of Demography Plots. Located in Virginia Basin, CO, USA.

Table 1. IPM Parameters. All parameters associated with the IPM model not previously stated

Variable	**Definition**
g	Germination rate (estimated from alpine plant literature) (Fernández-Pascual et al. 2021)
s_1	Seedling survival (estimated from extrapolated size-survival curve)
s_2	Year 1 juvenile survival (estimated with survival model evaluated at mean seedling size)
p_f	Probability of flowering
f_{se}	Number of seeds (flowers are counted, seeds per flower are estimated/counted once by D.W. Inouye)
C	Climate variable(s)
$f_1(z)$	Size distribution of recruits entering population
G(z'|z,C)	Growth kernel

Table 2. Climate Regression Terms. All terms are significant except for linear composite size term for the survival model. Student's t-distribution for growth had degree of freedom less than 30. The growth model had nonconstant variance which varied with composite size ($\sigma = -0.605 + 0.094$ (*composite* ¿¿).

Vital Rate	Family	Covariate	Lag (years)	Estimate
Survival	Logistic (binomial)	Intercept		1.626
Survival	Logistic (binomial)	Composite size		0.026
Survival	Logistic (binomial)	(Composite size)^2		-0.027
Survival	Logistic (binomial)	Snowpack	3	0.445
Survival	Logistic (binomial)	Spring temperature	4	-0.291
Survival	Logistic (binomial)	Summer temperature	1	-0.584
Growth	Student's t	Intercept		0.434
Growth	Student's t	Composite size		1.001
Growth	Student's t	Spring temperature	1	-0.093
Growth	Student's t	Spring temperature	2	-0.143
Growth	Student's t	Summer temperature	2	0.075
Reproduction	Logistic (binomial)	Intercept		-5.752
Reproduction	Logistic (binomial)	Composite size		1.430
Reproduction	Logistic (binomial)	Snowpack	4	-0.584
Reproduction	Logistic (binomial)	Spring temperature	0	-0.548
Reproduction	Logistic (binomial)	Summer temperature	0	0.273
Number of flowers	Poisson	Intercept		1.326
Number of flowers	Poisson	Composite size		0.184
Recruits	Gaussian	Intercept		-1.846
Recruits	Gaussian	Snowmelt	0	-0.239
Recruits	Gaussian	Snowmelt	1	-0.165

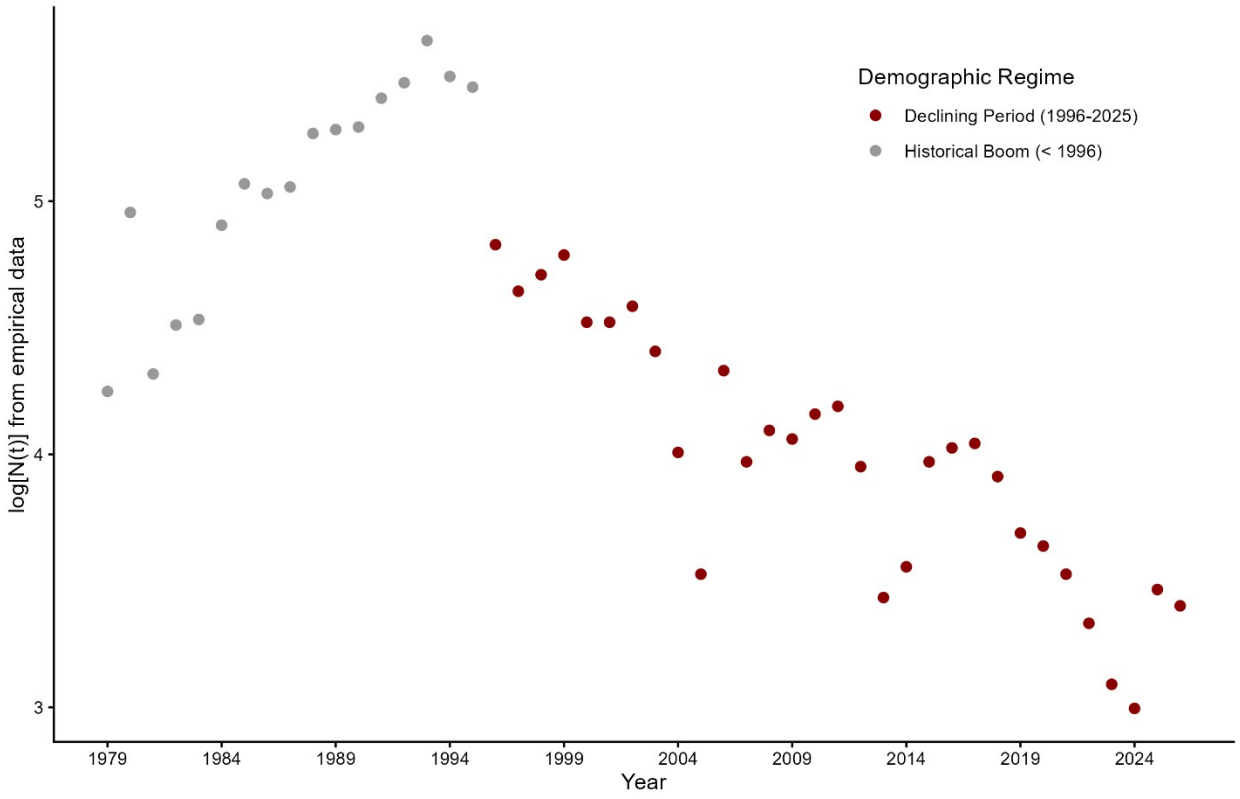

Figure 2. Empirical Population Size. Natural logarithm of the empirical population size over time. Regimes are separated by 1996, differentiating the increasing population size from the decreasing population size. Individuals perceived to be hidden in the Recruit Bank are not included.

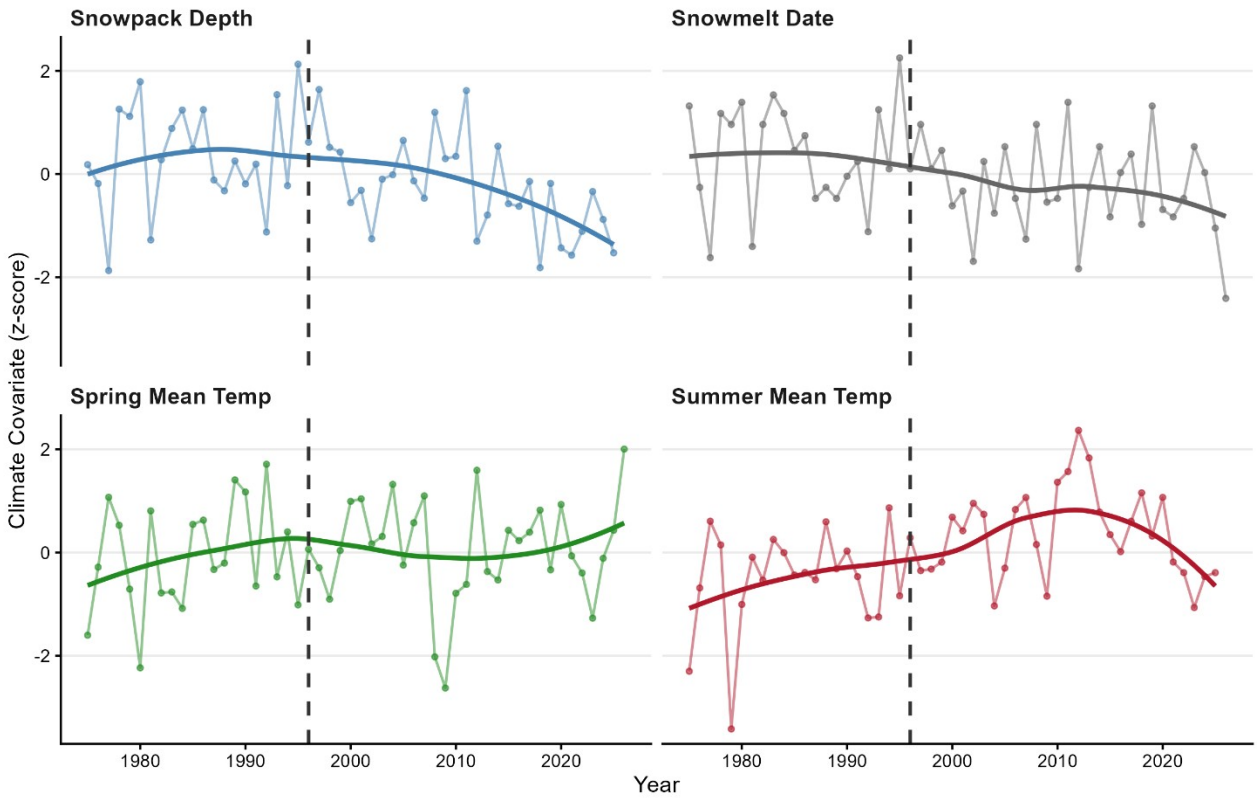

Figure 3. Climate Trends. Each climate variable is z-scaled. Snowpack depth and summer mean temperature is not included for 2026. The vertical line represents the change in demographic trends, when the population begins decreasing.

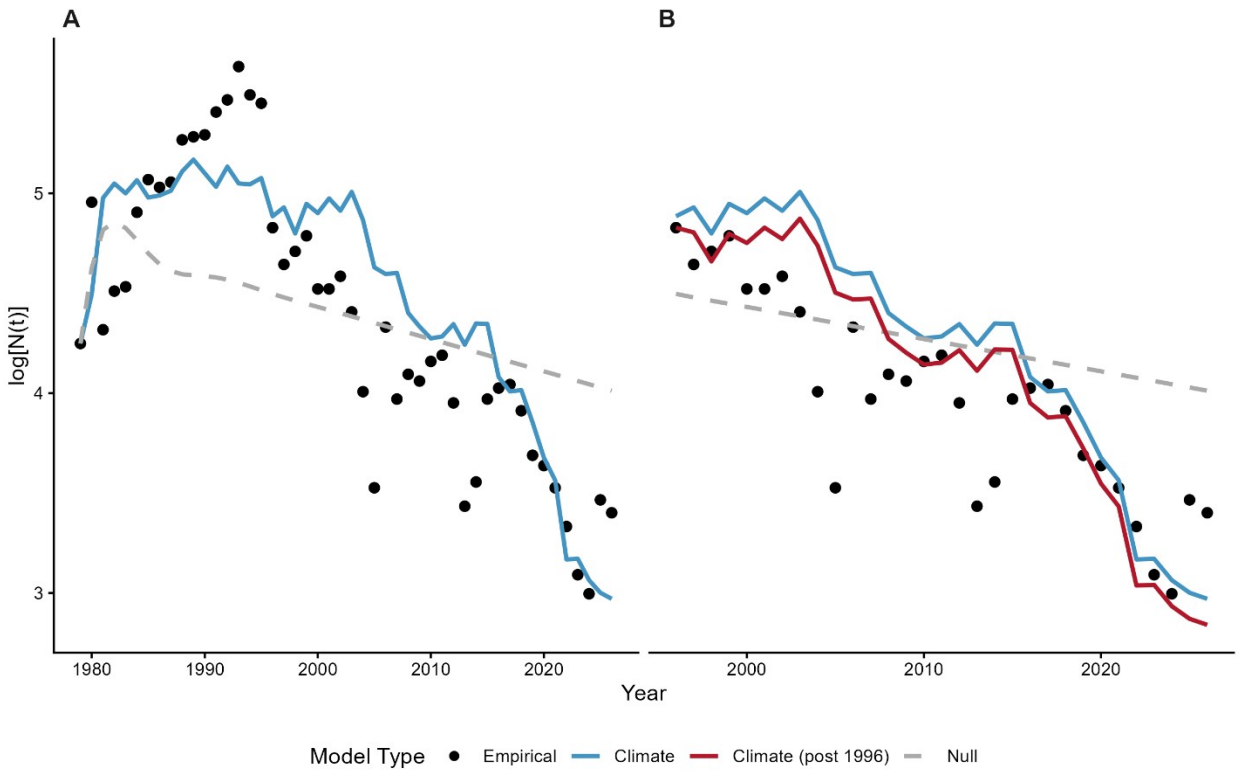

Figure 4. Hindcast Population Comparison. Empirical population abundance and IPM hindcasts across three models. Panel A includes the full dataset trajectory using the logarithm of the empirical population size (black dots), the stochastic mean-climate IPM hindcast (grey-dashed line), and the historic climate IPM (blue line). Panel B includes only 1996-2026 data, when the empirical population was declining. Re-initializing the historic climate IPM starting in 1996 (red line) reveals a closer match to the empirical population size.

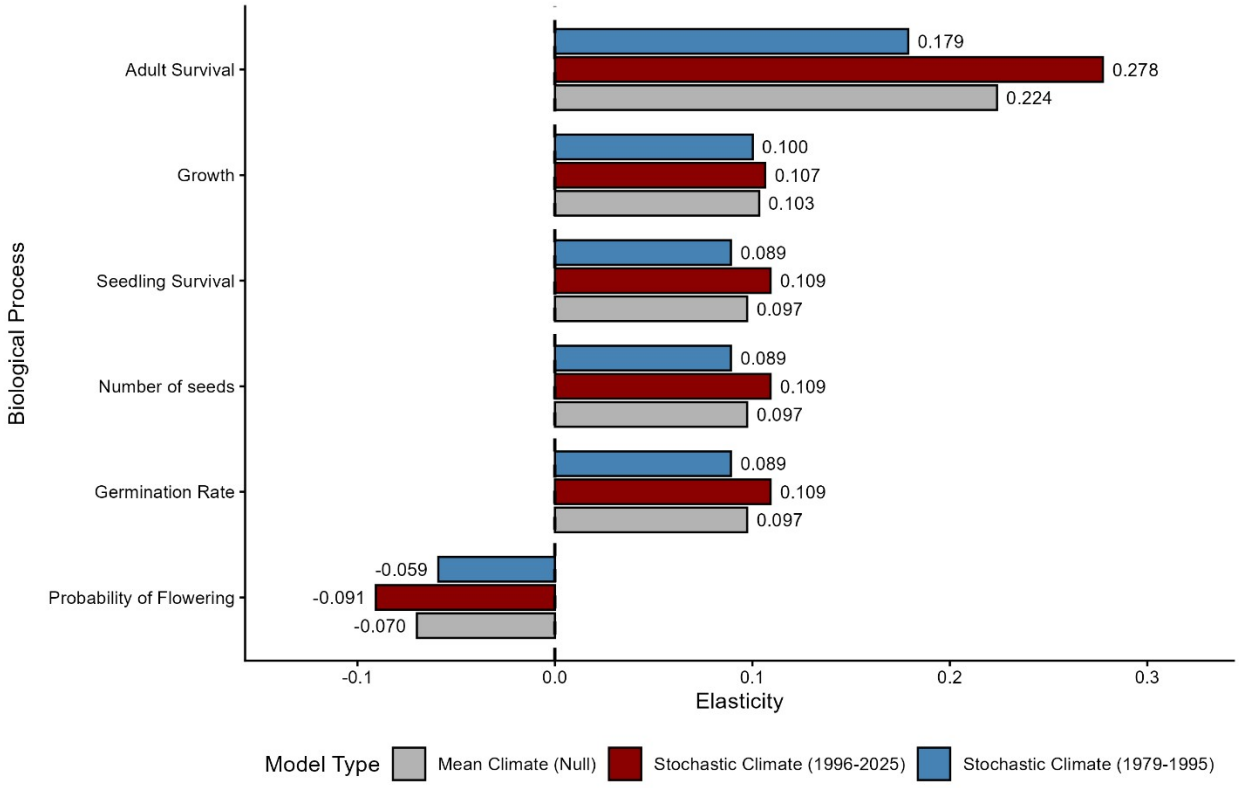

Figure 5. Elasticity Analyses. Elasticity analysis using a perturbation of δ=0.05 on each listed parameter. The mean climate elasticity used mean climate for all climate inputs. The stochastic climate elasticities used 200 iterations under the 1979-1995 and 1996-2025 climate regimes, respectively, to include environmental stochasticity.

References

Andrzejak, M., T. M. Knight, C. Plos, and L. Korell. 2025. Changes in reproduction mediate the effects of climate change and grassland management on plant population dynamics. Ecological Applications 35:e3063.

Arnold, T. W. 2010. Uninformative Parameters and Model Selection Using Akaike's Information Criterion. The Journal of Wildlife Management 74:1175–1178.

Bartoń, K. 2026. MuMIn: Multi-Model Inference. R.

Billings, W. D., and H. A. Mooney. 1968. The Ecology of Arctic and Alpine Plants. Biological Reviews 43:481–529.

Brooks, M. E., K. Kristensen, K. J. van Benthem, A. Magnusson, C. W. Berg, A. Nielsen, H. J. Skaug, M. Mächler, and B. M. Bolker. 2017. glmmTMB Balances Speed and Flexibility Among Packages for Zero-inflated Generalized Linear Mixed Modeling. The R Journal 9:378–400.

Burnham, K. P., and D. R. Anderson. 2002. Model Selection and Multimodel Inference: A Practical Information-Theoretic Approach. 2nd edition. Springer.

Cadotte, M. W., K. Carscadden, and N. Mirotchnick. 2011. Beyond species: functional diversity and the maintenance of ecological processes and services. Journal of Applied Ecology 48:1079–1087.

Campbell, D. R. 2019. Early snowmelt projected to cause population decline in a subalpine plant. Proceedings of the National Academy of Sciences 116:12901–12906.

Caswell, H. 2006. Matrix Population Models. Page Encyclopedia of Environmetrics. John Wiley & Sons, Ltd.

Che-Castaldo, J. P., and D. W. Inouye. 2011. The effects of dataset length and mast seeding on the demography of Frasera speciosa, a long-lived monocarpic plant. Ecosphere 2:art126.

Dalgleish, H. J., D. N. Koons, M. B. Hooten, C. A. Moffet, and P. B. Adler. 2011. Climate influences the demography of three dominant sagebrush steppe plants. Ecology 92:75–85.

Easterling, M. R., S. P. Ellner, and P. M. Dixon. 2000. Size-Specific Sensitivity: Applying a New Structured Population Model. Ecology 81:694–708.

Edwards, A. C., R. Scalenghe, and M. Freppaz. 2007. Changes in the seasonal snow cover of alpine regions and its effect on soil processes: A review. Quaternary International 162–163:172–181.

Ellis, S. L., and R. K. Shriver. 2026. A new normal? Population growth rates of a rare alpine plant stabilize after periods of decline, but not enough to allow for full population recovery. Biological Conservation 320:111898.

Ellner, S. P., D. Z. Childs, and M. Rees. 2016a. General Deterministic IPM. Pages 139–185 *in* S. P. Ellner, D. Z. Childs, and M. Rees, editors. Data-driven Modelling of Structured Populations: A Practical Guide to the Integral Projection Model. Springer International Publishing, Cham.

Ellner, S. P., D. Z. Childs, and M. Rees. 2016b. Environmental Stochasticity. Pages 187–227 *in* S. P. Ellner, D. Z. Childs, and M. Rees, editors. Data-driven Modelling of Structured Populations: A Practical Guide to the Integral Projection Model. Springer International Publishing, Cham.

Ellner, S. P., and M. Rees. 2006. Integral projection models for species with complex demography. American Naturalist 167:410–428.

Evers, S. M., T. M. Knight, D. W. Inouye, T. E. X. Miller, R. Salguero-Gómez, A. M. Iler, and A. Compagnoni. 2021. Lagged and dormant season climate better predict plant vital rates than climate during the growing season. Global Change Biology 27:1927–1941.

Fernández-Pascual, E., A. Carta, A. Mondoni, L. A. Cavieres, S. Rosbakh, S. Venn, A. Satyanti, L. Guja, V. F. Briceño, F. Vandelook, E. Mattana, A. Saatkamp, H. Bu, K. Sommerville, P. Poschlod, K. Liu, A. Nicotra, and B. Jiménez-Alfaro. 2021. The seed germination spectrum of alpine plants: a global meta-analysis. New Phytologist 229:3573–3586.

Fieberg, J., and S. P. Ellner. 2001. Stochastic matrix models for conservation and management: a comparative review of methods. Ecology Letters 4:244–266.

Freeman, B. G., M. N. Scholer, V. Ruiz-Gutierrez, and J. W. Fitzpatrick. 2018. Climate change causes upslope shifts and mountaintop extirpations in a tropical bird community. Proceedings of the National Academy of Sciences 115:11982–11987.

Grabherr, G., M. Gottfried, and H. Pauli. 2010. Climate Change Impacts in Alpine Environments. Geography Compass.

Grossiord, C., T. N. Buckley, L. A. Cernusak, K. A. Novick, B. Poulter, R. T. W. Siegwolf, J. S. Sperry, and N. G. McDowell. 2020. Plant responses to rising vapor pressure deficit. New Phytologist 226:1550–1566.

Hastings, A. 2004. Transients: the key to long-term ecological understanding? Trends in Ecology & Evolution 19:39–45.

Iler, A. M., A. Compagnoni, D. W. Inouye, J. L. Williams, P. J. CaraDonna, A. Anderson, and T. E. X. Miller. 2019a. Reproductive losses due to climate change-induced earlier flowering are not the primary threat to plant population viability in a perennial herb. Journal of Ecology 107:1931–1943.

Iler, A. M., A. Compagnoni, D. W. Inouye, J. L. Williams, P. J. CaraDonna, A. Anderson, and T. E. X. Miller. 2019b. Reproductive losses due to climate change-induced earlier flowering

are not the primary threat to plant population viability in a perennial herb. Journal of Ecology 107:1931–1943.

Inouye, D. W. 2008. Effects of Climate Change on Phenology, Frost Damage, and Floral Abundance of Montane Wildflowers. Ecology 89:353–362.

Inouye, D. W. 2020. Effects of climate change on alpine plants and their pollinators. Annals of the New York Academy of Sciences 1469:26–37.

Janeček, Š., A. Bartušková, M. Bartoš, J. Altman, F. de Bello, J. Doležal, V. Latzel, V. Lanta, J. Lepš, and J. Klimešová. 2015. Effects of disturbance regime on carbohydrate reserves in meadow plants. AoB PLANTS 7:plv123.

Kagawa, O., S. K. Hirota, T. Hirano, K. Kimura, G. Kobayashi, Y. Suyama, S. Chiba, and D. Yamazaki. 2024. The population structure and demography of an intertidal gastropod Lunella correensis around the Japanese Archipelago affected by past environmental change. Marine Biology 171:177.

Körner, C., and E. Hiltbrunner. 2021. Why Is the Alpine Flora Comparatively Robust against Climatic Warming? Diversity 13:383.

Kosolapova, A., and I. Altshuler. 2024. Effects of reduced snowpack due to climate warming on abiotic and biotic soil properties in alpine and boreal forest systems. PLOS Climate 3:e0000417.

Kotlarski, S., A. Gobiet, S. Morin, M. Olefs, J. Rajczak, and R. Samacoïts. 2023. 21st Century alpine climate change. Climate Dynamics 60:65–86.

Lesica, P., and B. McCune. 2004. Decline of arctic-alpine plants at the southern margin of their range following a decade of climatic warming. Journal of Vegetation Science 15:679–690.

Levin, S. C., D. Z. Childs, A. Compagnoni, S. Evers, T. M. Knight, and R. Salguero-Gómez. 2021. ipmr: Flexible implementation of Integral Projection Models in R. Methods in Ecology and Evolution 12:1826–1834.

Matteodo, M., S. Wipf, V. Stöckli, C. Rixen, and P. Vittoz. 2013. Elevation gradient of successful plant traits for colonizing alpine summits under climate change. Environmental Research Letters 8:024043.

Merow, C., J. P. Dahlgren, C. J. E. Metcalf, D. Z. Childs, M. E. K. Evans, E. Jongejans, S. Record, M. Rees, R. Salguero-Gómez, and S. M. McMahon. 2014. Advancing population ecology with integral projection models: a practical guide. Methods in Ecology and Evolution 5:99–110.

Metcalf, J. C., K. E. Rose, and M. Rees. 2003. Evolutionary demography of monocarpic perennials. Trends in Ecology & Evolution 18:471–480.

Miller, T. E. X., and S. P. Ellner. 2025. My, how you've grown: A practical guide to modeling size transitions for integral projection model (IPM) applications. Ecology 106:e70088.

National Park Service. 2024. Yellow & Orange Flowers - Rocky Mountain National Park (U.S. National Park Service). https://www.nps.gov/romo/learn/nature/yellow_orange_flowers.htm.

Nomoto, H. A., and J. M. Alexander. 2021. Drivers of local extinction risk in alpine plants under warming climate. Ecology Letters 24:1157–1166.

Oberbauer, S. F., and W. D. Billings. 1981. Drought tolerance and water use by plants along an alpine topographic gradient. Oecologia 50:325–331.

Oldfather, M. F., and D. D. Ackerly. 2019. Microclimate and demography interact to shape stable population dynamics across the range of an alpine plant. New Phytologist 222:193–205.

Palacio, S., A. Lenz, S. Wipf, G. Hoch, and C. Rixen. 2015. Bud freezing resistance in alpine shrubs across snow depth gradients. Environmental and Experimental Botany 118:95–101.

Prather, R. M., N. Underwood, R. M. Dalton, B. Barr, and B. D. Inouye. 2023. Climate data from the Rocky Mountain Biological Laboratory (1975–2022). Ecology 104:e4153.

R Core Team. 2025. R: A Language and Environment for Statistical Computing. R Foundation for Statistical Computing.

Ramula, S., M. Rees, and Y. M. Buckley. 2009. Integral projection models perform better for small demographic data sets than matrix population models: a case study of two perennial herbs. Journal of Applied Ecology 46:1048–1053.

Rees, M., and S. P. Ellner. 2009. Integral projection models for populations in temporally varying environments. Ecological Monographs 79:575–594.

Tenhumberg, B., E. E. Crone, S. Ramula, and A. J. Tyre. 2018. Time-lagged effects of weather on plant demography: drought and Astragalus scaphoides. Ecology 99:915–925.

Thornton, P. K., P. J. Ericksen, M. Herrero, and A. J. Challinor. 2014. Climate variability and vulnerability to climate change: a review. Global Change Biology 20:3313–3328.

Tuljapurkar, S. 1990. Population Dynamics in Variable Environments. Lecture Notes in Biomathematics.

de Valpine, P., and J. Harte. 2001. Plant Responses to Experimental Warming in a Montane Meadow. Ecology 82:637–648.

Williams, J. L., H. Jacquemyn, B. M. Ochocki, R. Brys, and T. E. X. Miller. 2015. Life history evolution under climate change and its influence on the population dynamics of a long-lived plant. Journal of Ecology 103:798–808.

Winkler, D. E., R. J. Butz, M. J. Germino, K. Reinhardt, and L. M. Kueppers. 2018. Snowmelt Timing Regulates Community Composition, Phenology, and Physiological Performance of Alpine Plants. Frontiers in Plant Science 9.

Wipf, S., V. Stoeckli, and P. Bebi. 2009. Winter climate change in alpine tundra: plant responses to changes in snow depth and snowmelt timing. Climatic Change 94:105–121.